九州大学大学院総合理工学報告
第 47 巻 第 1 号 1-8 頁 令和 7 年 9 月

Engineering Sciences Reports, Kyushu University
Vol. 47, No. 1, pp. 1-8, SEP, 2025

Photochemical Removal of C_2H_4 in N_2 or Air by Using a 172 nm Xe_2 Excimer Lamp at Atmospheric Pressure

Masaharu TSUJI,[*1,2†] Naohiro KAMO[*3] and Masato MIYANO[*3]
[†]E-mail of corresponding author: tsuji@cm.kyushu-u.ac.jp

(Received February 14, 2025, accepted February 28, 2025)

The photochemical removal of ethylene was investigated in N_2 or air using a head-on or side-on type of 172 nm vacuum ultraviolet (VUV) Xe_2 excimer lamp at atmospheric pressure. C_2H_4 was selectively converted to 1-butene via photo-dimerization reaction in N_2, whereas C_2H_4 was finally oxidized to CO_2 via HCHO, HCOOH, and CO intermediates in air. When the head-on lamp was replaced with the side-on one with a larger irradiation area, the removal rate of C_2H_4 in air was increased by a factor of 8.2. It was found that the $O(^3P) + C_2H_4$ reaction plays a major role in the initial stage of the oxidation of C_2H_4 under 172 nm VUV irradiation in air. Major reaction pathways from C_2H_4 to 1-butene or CO_2 under 172 nm VUV photolysis in N_2 or air are discussed.

Key words: *VUV photolysis, 172 nm Xe_2 excimer lamp, C_2H_4, $O(^3P)$ atoms, O_3, 1-butene. Dimerization, Oxidation, CO_2, Air, Atmospheric pressure*

1. Introduction

Ethylene is a plant hormone, which evolves from fruits and vegetables and accelerates ripening in stored postharvest fruits and vegetables.[1,2] The presence of a small amount of C_2H_4 causes premature spoilage and substantial food waste in industry. Therefore, removal of C_2H_4 during storage of fruits and vegetables is required to extend their freshness date.

Extensive studies have been conducted using effective and economically reasonable techniques for elimination of C_2H_4 from air during storage of fruits and vegetables. Conventional C_2H_4 removal techniques are air ventilation, low-temperature storage,[3] the use of different adsorber/absorbers,[4] the use of potassium permanganate ($KMnO_4$),[5] and ozone and catalytic oxidation.[6] UV and/or VUV photolysis is an emerging technique for C_2H_4 postharvest management.[7,8] Photolysis generally employs UV light sources, such as low-pressure and medium-pressure mercury lamps with approximately 85% output UV light at 254 nm and 15% output VUV light at 185 nm. This technique has demonstrated promising C_2H_4 removal capabilities and was successful in prolonging the shelf-life of apples and fruits.

We have recently used 172 nm VUV excimer lamps to remove such hydrocarbons and aldehydes as CH_4, C_6H_6, CH_3CHO, and C_2H_3CHO.[9-14] They could efficiently be decomposed and oxidized to CO_2 in air at atmospheric pressure without using any expensive noble-metal catalysts. In the present study, we attempted to use a 172 nm Xe_2 excimer lamp as a new photochemical removal method of C_2H_4 in air at atmospheric pressure.

Previous photolysis of C_2H_4 was carried out by using a mixture of 254 nm + 185 nm light in air.[1,2,7,8] The threshold wavelengths for the formation of $O(^3P)$ and $O(^1D)$ from photolysis of O_2 are as follows.[15]

$$O_2 + h\nu\ (\leq 242.4\ \text{nm}) \rightarrow O(^3P) + O(^3P) \quad (1)$$
$$O_2 + h\nu\ (\leq 175.0\ \text{nm}) \rightarrow O(^3P) + O(^1D) \quad (2)$$

On the basis of these facts, O_2 cannot be decomposed into $O(^3P) + O(^3P)$ at 254 nm, whereas it can be decomposed into $O(^3P) + O(^3P)$ at 185 nm with a small absorption cross section.[15]

$$O_2 + h\nu\ (185\ \text{nm}) \rightarrow O(^3P) + O(^3P) \quad (3)$$
$$\sigma_3 \approx 3.3 \times 10^{-20}\ \text{cm}^2\ \text{molecule}^{-1}$$

On the other hand, O_2 is selectively decomposed into $O(^1D) + O(^3P)$ at 172 nm with a larger absorption cross section.[15,16]

*1 Institute for Materials Chemistry and Engineering, and Research and Education Center of Green Technology
*2 Department of Applied Science for Electronics and Materials
*3 Department of Applied Science for Electronics and Materials, Graduate Student

$$O_2 + h\nu\ (172\ nm) \rightarrow O(^1D) + O(^3P) \qquad (4)$$
$$\sigma_4 \approx 4.63 \times 10^{-19}\ cm^2\ molecule^{-1}$$

Since absorption cross section of (4) is 14 times larger than that of (3), 172 nm light is expected to be more suitable than 185 nm one for C_2H_4 removal. In addition, the inert rare gas lamp is a more eco-friendly light source than the toxic mercury lamp. Therefore, mercury-free process is strongly desired as a practical photochemical removal technique.

The major purpose of this study is to obtain fundamental information on photochemical reactions of C_2H_4 under irradiation of 172 nm Xe_2 excimer lamps in air. Not only direct VUV photochemical reactions of C_2H_4, but also reactions of $O(^3P,^1D)$ and O_3 with C_2H_4 may contribute to the removal of C_2H_4. To examine effects of direct VUV photochemical reactions, C_2H_4 is decomposed in N_2.

Major photochemical reaction pathways of C_2H_4 in N_2 or air are discussed. All reaction rate constants and branching ratios of products used for discussion have been measured at about 300 K.[17]

2. Experimental

VUV photolysis apparatus used in this work was the same as that reported previously.[10,11] Lights from an unfocused head-on type or side-on type 172 nm Xe_2 lamp were used to remove C_2H_4 at room temperature. Most experiments were conducted using the head-on lamp (input power 20 W, irradiance 50 mW/cm^2, UER20H172; Ushio Inc). In addition, the side-on lamp (input power 20 W, irradiance 10 mW/cm^2, UER20H172; Ushio Inc) was used.

Experiments were carried out in a closed batch system. The total pressure was maintained at atmospheric pressure and the C_2H_4 concentration was 500 or 714 ppm in the experiments using the head-on or side-on lamps, respectively. Sample gases before and after photoirradiation were analyzed by a HORIBA gas analysis system (FG122-LS) equipped with an FTIR spectrometer. The IR spectra were measured in the 980–4000 cm^{-1} region with an optical resolution of 4 cm^{-1}. The concentrations of C_2H_4, HCHO, HCOOH, CO, CO_2, and O_3 were determined from peak intensities of each FTIR band. The concentrations of C_2H_4, HCHO, CO, and CO_2 were calibrated using their standard samples supplied from gas companies. The concentrations of O_3 and HCOOH were evaluated by reference to the standard spectral data supplied by HORIBA Ltd.

The following gases were used without further purification: N_2 (Taiyo Nissan Inc.: purity >99.9998%), O_2 (Nippon Sanso Inc.: >99.99995%), C_2H_4 (Nippon Sanso Inc.: 3000 ppm in high purity N_2). C_2H_4 was diluted in N_2 or air (20% O_2) before use.

3. Results and discussion

3.1 C_2H_4 removal in N_2

C_2H_4 removal in N_2 was attempted using a head-on lamp. N_2 has no absorption at 172 nm.[15] On the other hand, C_2H_4 absorbs 172 nm photons with an absorption cross section of 1.2×10^{-17} cm^2 molecule^{-1}.[18] Therefore, photochemical removal of C_2H_4 by 172 nm VUV light may be possible in a C_2H_4/N_2 mixture. Figures 1(a)–1(d) show FTIR spectra of C_2H_4 (500 ppm) in N_2 before and after photoirradiation for 1, 3, and 5 min, respectively. Before photoirradiation, we can identify a strong C_2H_4 band in the 980–1100 cm^{-1} region with a peak at 995 cm^{-1} and a weak C_2H_4 band in the 2900–3200 cm^{-1} region with a peak at 2989 cm^{-1} (Fig. 1(a)).[19] After photoirradiation for 1 min, the main C_2H_4 band reduces its intensity by 28% (Fig. 1(b)). It should be noted that a weak new peak appears near 3000 cm^{-1} region. By comparison with reported IR spectra of isomers of butenes,[19] it was ascribed to 1-butene band. The formation of 1-butene by VUV photolysis of C_2H_4 at 147 nm had been reported by Hara et al.[20]

Figure 2 shows the dependence of concentrations of C_2H_4 and 1-C_4H_8 on the irradiation time in the 0–10 min range. The C_2H_4 concentration decreases from 500 ppm to 200 ppm with increasing the irradiation time in the 0–5 min range, whereas the 1-C_4H_8 concentration increases from zero ppm to about 150 ppm in the same time range. Thus, photo-dimerization dominantly occurs in this time range. It should be noteworthy that the concentrations of C_2H_4 and 1-C_4H_8 are essentially independent on the irradiation time in the 5–10 min range. On the basis of above findings, forward photochemical dimerization reaction leading to 1-C_4H_8 and backward photodissociation reaction leading to C_2H_4 reactant equilibrate with each other under 172 nm photoirradiation in N_2 after 5 min irradiation.

$$2C_2H_4 \underset{+\ h\nu\ (172\ nm)}{\overset{+\ h\nu\ (172\ nm)}{\rightleftharpoons}} 1\text{-}C_4H_8 \qquad (5)$$

More detailed reaction mechanism is discussed in Sec. 3.3.1.

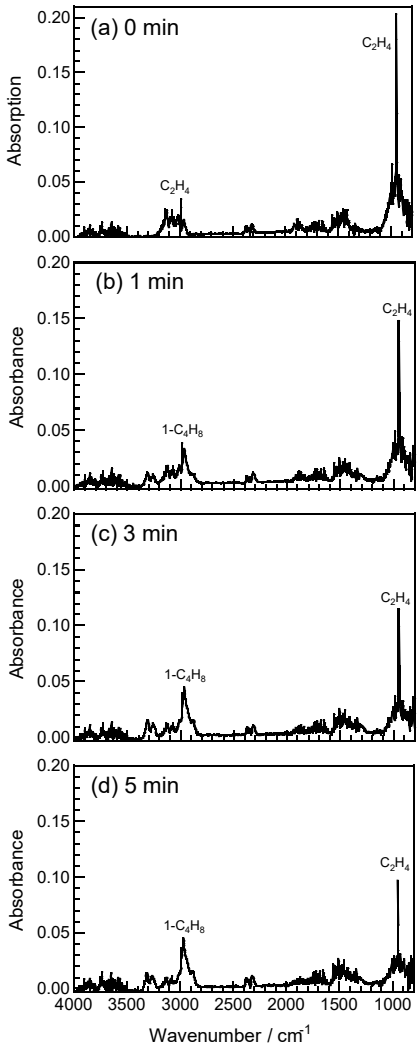

Fig. 1. (a) FTIR spectra of C_2H_4 in N_2 (a) before photoirradiation and (b)–(d) after photoirradiation for 1, 3, and 5 min, respectively. Spectra were measured using a head-on lamp.

3.2 C_2H_4 removal in air

C_2H_4 removal in air was examined using head-on and side-on lamps. Figures 3(a)–3(d) show FTIR spectra of C_2H_4 (500 ppm) in air (20% O_2) before and after photoirradiation for 1, 3, and 5 min, respectively. These spectra were measured using the head-on lamp. Before photoirradiation, strong and weak C_2H_4 bands are observed in the 980–1100 cm^{-1} and 2900–3200 cm^{-1} regions, respectively. After photoirradiation for 1 min, the C_2H_4 peak reduced its intensity by 66%, whereas new CO_2,

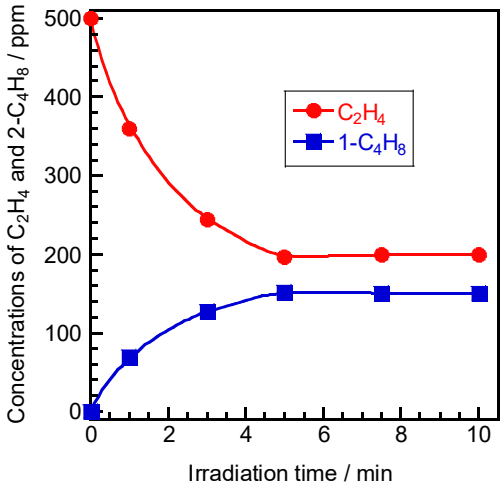

Fig. 2. Dependence of concentrations of C_2H_4 and 1-C_4H_8 in N_2 on the irradiation time measured using a head-on lamp.

CO, HCHO, HCOOH, and O_3 bands are observed. With increasing the photoirradiation time from 1 min to 5 min, the C_2H_4 peak disappears, and the intensities of CO_2 and O_3 bands increase, whereas CO, HCHO, and HCOOH bands decrease.

Figure 4 shows the dependence of concentrations of C_2H_4, CO, CO_2, HCHO, HCOOH, and O_3 on the irradiation time in the 0–10 min range. The concentration of C_2H_4 rapidly decreases from 500 ppm to 48 ppm with increasing the irradiation time until 2 min, and then slowly decreases to zero at 5 min. The concentration of CO increases to 525 ppm until 3 min, and then slowly decreases to 440 ppm in the 3–10 min range. The concentration of CO_2 increases almost linearly to 753 ppm until 10 min. The concentrations of HCHO and HCOOH increase to 101 and 242 ppm at 1 min, and then slowly decrease in the 1–10 min range. These time profiles suggest that CO, HCHO, and HCOOH are slowly converted to CO_2 under the operation condition. The concentration of O_3 increases to 2.4% after 10 min.

Figures 5(a)–5(d) show FTIR spectra of C_2H_4 (714 ppm) in air before and after photoirradiation for 5, 30, and 90 s, respectively. These spectra were obtained using the side-on lamp. Before photoirradiation, C_2H_4 bands are observed in the 980–1100 cm^{-1} and 2900–3200 cm^{-1} regions. It should be noteworthy that the removal rate of C_2H_4 is strongly enhanced by using the side-on lamp. After photoirradiation for only 5 s, the C_2H_4 peak reduced its intensity by 52%, whereas new CO_2, CO, HCHO,

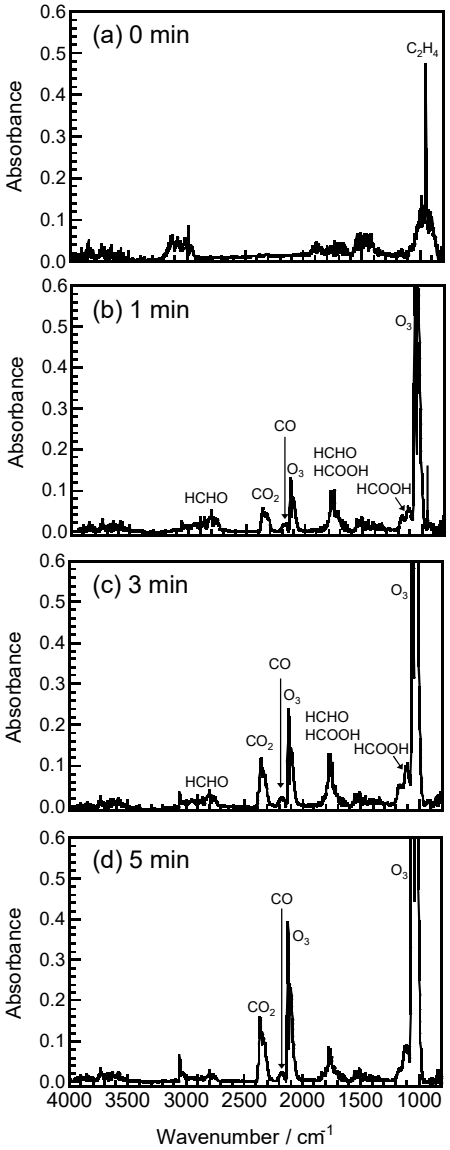

Fig. 3. (a) FTIR spectra of C_2H_4 in air (a) before photoirradiation and (b)–(d) after photoirradiation for 1, 3, and 5 min, respectively. Spectra were measured using a head-on lamp.

HCOOH, and O_3 bands appear. With increasing the photoirradiation time from 5 s to 30 s, the C_2H_4 peak disappears and the intensities of HCOOH, CO_2 and O_3 bands increase. At 90 s CO_2 and O_3 bands further increase, whereas CO, HCHO, and HCOOH bands become weak.

Figure 6(a) shows the dependence of concentrations of C_2H_4, CO, CO_2, HCHO, HCOOH, and O_3 on the irradiation time in the 0–300 s range. An expanded plot below 100 s is given in Fig. 6(b), where variations of

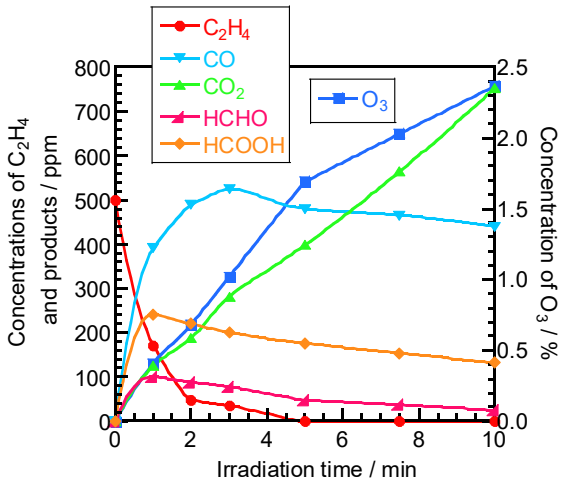

Fig. 4. Dependence of concentrations of C_2H_4, products, and O_3 in air on the irradiation time measured using a head-on lamp.

concentrations of C_2H_4 and HCHO at short times can be confirmed. It should be noted that the concentration of C_2H_4 rapidly decreases to zero after only 15 s irradiation. The concentrations of HCHO and HCOOH have peaks at 10 s and 30 s, respectively. The maximum concentration of HCOOH is 3.4 times higher than that of HCHO. The concentrations HCHO and HCOOH become zero at 45 s and 90 s, respectively. The concentrations of CO increase to 663 ppm in the 0–30 s range and then slowly decrease to zero in the 30–300 s range. The concentration of CO_2 rapidly increases to 540 ppm until 90 s and slowly increases to 628 ppm in the 90–300 s range. These time profiles of products suggest that major oxidation of C_2H_4 occur through HCHO → HCOOH → CO → CO_2. The concentration of O_3 rapidly increases to 1.7% in the 0–90 s range and then slowly increases to 1.9% in the 90–300 s range.

The initial pseudo-first-order decomposition rate of C_2H_4 by using the side-on lamp in the 0–10 s range (0.159 s^{-1}) is 8.2 times faster than that by using the head-on lamp in the 0–120 s range (0.0195 s^{-1}). The window area of the side-on lamp, from which VUV enters into the photolysis chamber, is 9.8 times wider than that of the head-on one.[10,11] Therefore, the fraction of photoirradiation volume in the reaction chamber at 20% O_2 increases from 4.3% to 33.3% by changing excimer lamp from the head-on type to the side-on one.[11] This is a major reason for the significant enhancement of removal rate of C_2H_4 using the side-on lamp.

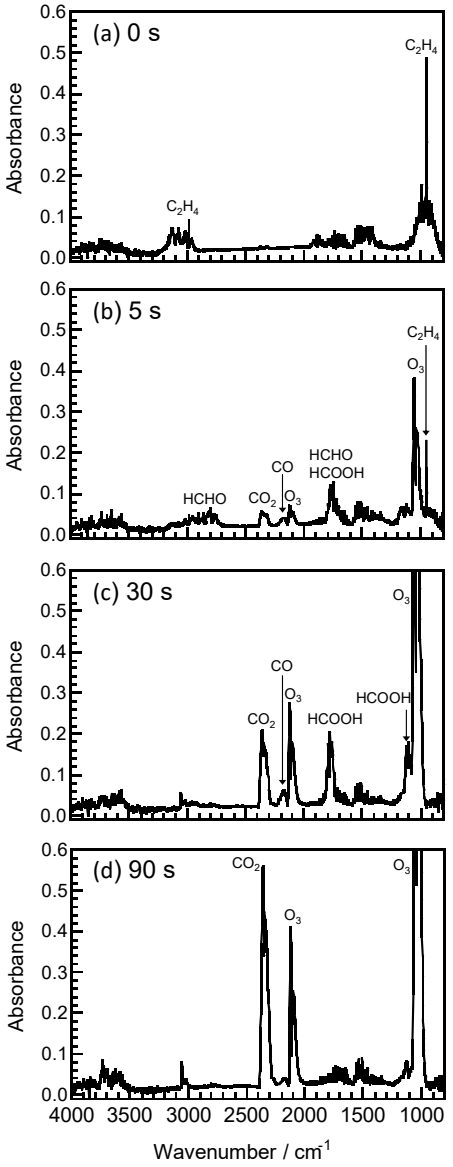

Fig. 5. (a) FTIR spectra of C_2H_4 in air (a) before photoirradiation and (b)–(d) after photoirradiation for 5, 30, and 90 s, respectively. Spectra were measured using a side-on lamp.

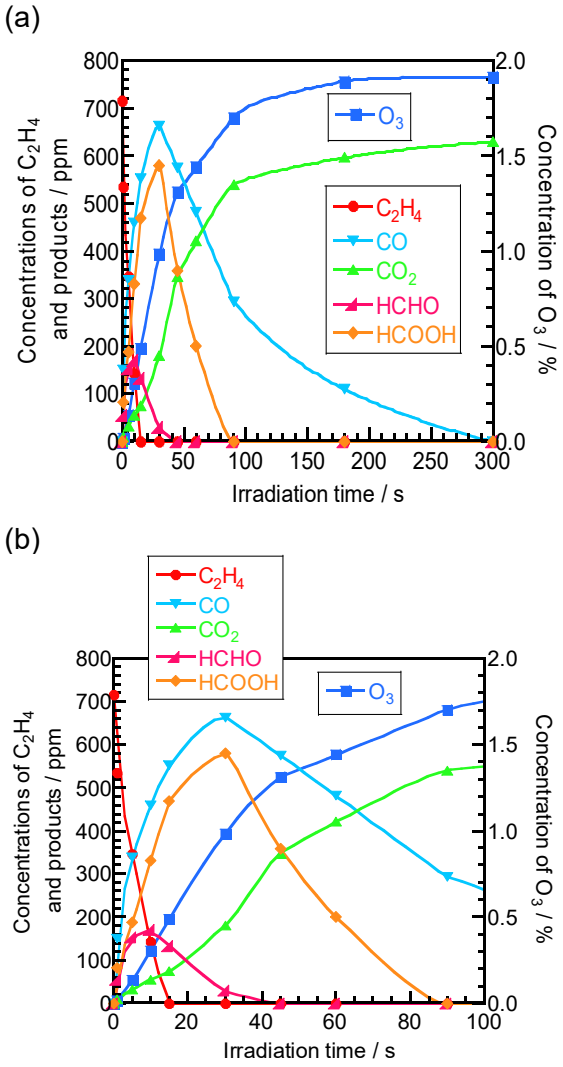

Fig. 6. Dependence of concentrations of C_2H_4, products, and O_3 in air on the irradiation time measured using a side-on lamp in the (a) 0–300 s and (b) 0–100 s ranges.

3.3 Possible removal mechanisms of C_2H_4 under 172 nm photolysis in N_2 or air

3.3.1 C_2H_4 Removal Mechanism in N_2

We found that 1-C_4H_8 is selectively formed by 172 nm VUV photolysis of C_2H_4 in N_2. The most probable formation and decomposition processes of 1-C_4H_8 are as follows.

$$C_2H_4 + h\nu\ (172\ nm) \rightarrow C_2H_4^* \quad (6)$$
$$C_2H_4^* + C_2H_4 \rightarrow 1\text{-}C_4H_8 \quad (7)$$
$$1\text{-}C_4H_8 + h\nu\ (172\ nm) \rightarrow 1\text{-}C_4H_8^* \quad (8)$$
$$1\text{-}C_4H_8^* \rightarrow C_2H_4 + C_2H_4 \quad (9)$$

Experimental data suggest that the formation and decomposition of 1-C_4H_8 under 172 nm photoirradiation become equilibrium after 5 min irradiation. FTIR data indicated that 1-C_4H_8 is selectively formed and no 2-C_4H_8 is produced in process (7).

3.3.2 C_2H_4 Removal Mechanism of in Air

Under 172 nm photolysis of C_2H_4 (500 or 714 ppm) in an N_2/O_2 mixture (20% O_2), the 172 nm light is absorbed by C_2H_4 and O_2. In general, the total photon energy absorbed by such a mixture as C_2H_4 and O_2 during passing through the decomposition chamber, E_{total}, was calculated from the relation:

$$E_{total} = E_0 - E_0\, exp(-l \sum_i \sigma_i N_i) \quad (10)$$

Here, E_0, l, σ_i, and N_i are the energy of excimer lamp, the length of decomposition chamber, absorption cross section of a molecule i, and its number density, respectively. Photon energy absorbed by a molecule i, E_i, is obtained from the relation.

$$E_i = E_{total} \times \frac{\sigma_i N_i}{\sum_i \sigma_i N_i} \quad (11)$$

$\sigma_{C_2H_4}$ and σ_{O_2} values at 172 nm were reported to be 1.2×10^{-17} and 4.63×10^{-19} cm^2 molecule^{-1}, respectively.[15,18] When we calculated $E_{C_2H_4}$ / ($E_{C_2H_4}$ + E_{O_2}) and E_{O_2} / ($E_{C_2H_4}$ + E_{O_2}) values at 172 nm using these values at C_2H_4 concentrations of 500 and 714 ppm, they are 6.1 and 93.9% and 8.5 and 91.5%, respectively. These values suggest that most photons are initially absorbed by O_2, because the O_2 concentration is 400 and 280 times higher than C_2H_4 at 500 and 714 ppm, respectively. Thus, photolysis of C_2H_4 in air starts from selective photolysis of O_2 into $O(^1D)$ + $O(^3P)$ under 172 nm photoirradiation, as shown in reaction (4). Metastable $O(^1D)$ atoms are rapidly quenched to the ground $O(^3P)$ atoms by collisions with N_2 and O_2 atoms in air.

$$O(^1D) + N_2 \rightarrow O(^3P) + N_2 \quad (12)$$
($k_{12} = 2.6 \times 10^{-11}$ cm^3 molecule^{-1} s^{-1})[17]

$$O(^1D) + O_2 \rightarrow O(^3P) + O_2 \quad (13)$$
($k_{13} = 4.0 \times 10^{-11}$ cm^3 molecule^{-1} s^{-1})[17]

The rate constants and product branching ratios of the $O(^3P)/C_2H_4$ reaction have been measured.[17,21]

$$O(^3P) + C_2H_4$$
$$\rightarrow CH_3 + CHO \quad 0.53 \pm 0.04 \quad (14a)$$
$$\rightarrow CH_2CHO + H \quad 0.39 \pm 0.10 \quad (14b)$$
$$\rightarrow CH_2 + CH_2O \quad 0.06 \pm 0.03 \quad (14c)$$
$$\rightarrow CH_2CO + H_2 \quad 0.019 \pm 0.001 \quad (14d)$$
($k_{14} = 7.25 \times 10^{-13}$ cm^3 molecule^{-1} s^{-1})

This implies that major primary products involving carbon atom are CH_3, CHO, and CH_2CHO. The rate constant and products of the $O(^1D)/C_2H_4$ reaction have been measured.[17,21-25]

$$O(^1D) + C_2H_4 \rightarrow C_2H_3 + OH \quad (15a)$$
$$\rightarrow CH_2CHOH \quad (15b)$$
$$\rightarrow C_2H_4O \quad (15c)$$
($k_{15} = 2.19 \times 10^{-10}$ cm^3 molecule^{-1} s^{-1})

The main channels of the $O(^1D)/C_2H_4$ reaction are H abstraction reactions leading to C_2H_3 + OH radicals and C−H insertion channel to form highly excited vinylalcohol.[22,23] It has also been predicted that the ethylene oxide is formed through a barrierless reaction channel (15c).[24] Although Miyoshi *et al.*[25] evaluated the branching ratio of (15a) to be 0.54±0.03, branching ratios of reactions (15b) and (15c) have not been reported. The $O(^1D)/C_2H_4$ reaction is faster than the $O(^3P)/C_2H_4$ reaction by a factor of 302. However, the initial concentration of C_2H_4 (714 ppm) is much smaller than those of N_2 (80%) and O_2 (20%). When the relative contribution of the $O(^1D)/C_2H_4$ reaction (15) to quenching reactions (12) + (13) is evaluated using rate constants and initial concentrations, it is smaller than that of the latter ones by a factor of 184. Therefore, it is expected that the $O(^1D)/C_2H_4$ reaction is insiginificant for the C_2H_4 removal in air under the present experimental condition.

We have recently studied CH_4 removal in air using the same apparatus and a similar initial CH_4 concentration (730 ppm) as that of C_2H_4 in this study.[14] In the case of CH_4, major active species for the decomposition of CH_4 is $O(^1D)$ with an excitation energy of 1.967 eV.[15] The rate constant of the $O(^1D)/CH_4$ reaction is 32% smaller than that of the $O(^1D)/C_2H_4$ reaction.

$$O(^1D) + CH_4 \rightarrow \text{products} \quad (16)$$
($k_{16} = 1.50 \times 10^{-10}$ cm^3 molecule^{-1} s^{-1})[17]

In the case of CH_4 removal by $O(^1D)$ using the side-on lamp, it takes about 45 min for the complete removal of CH_4 in air.[14] On the other hand, it takes only 15 s for the complete removal of C_2H_4. This fact also supports that major active species is not minor $O(^1D)$ atoms but major $O(^3P)$ atoms in the case of the C_2H_4 removal in air.

O_3 molecules are formed through the following three-body recombination reactions.

$$O + O_2 + N_2 \rightarrow O_3 + N_2$$
($k_{17a} = 6.01 \times 10^{-34}$ cm^6 molecule^{-2} s^{-1})[17] (17a)

$$O + O_2 + O_2 \rightarrow O_3 + O_2$$
($k_{17b} = 6.20 \times 10^{-34}$ cm^6 molecule^{-2} s^{-1})[17] (17b)

It is known that the rate constant of O_3 with C_2H_4 is very small at 298 K.

$$O_3 + C_2H_4 \rightarrow \text{Products}$$
(1.55×10^{-18} cm^3 molecule^{-1} s^{-1})[17] (18)

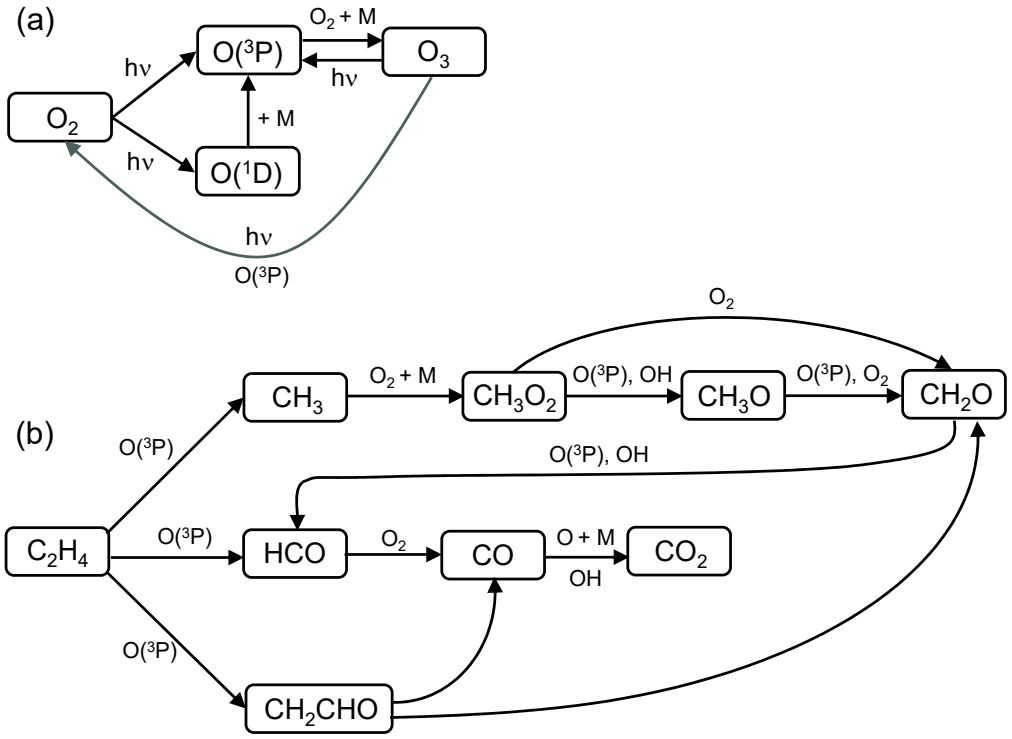

Scheme 1. (a) photolysis of O_2 and O_3 under 172 nm VUV irradiation. (b) Major oxidation processes of C_2H_4 under 172 nm VUV photolysis in air. M denotes the third-body N_2 and O_2 molecules.

Therefore, O_3 will be unimportant active species in the C_2H_4 removal in the intial stage. As shwon in Fig. 6, fast removal of C_2H_4 occurs just after irradiation of 172 nm light, where the concentration of O_3 is very low. This experimental observation supports the fact that O_3 molecules do not participate in the C_2H_4 removal in the intial stage.

Scheme 1(a) shows 172 nm photolysis of O_2 and O_3 in air. $O(^3P)$ atoms, which are dominant active species for C_2H_4 removal, are formed by photolysis of O_2 and O_3 and collisional quenching of $O(^1D)$. On the basis of known oxidation reactions of such major initial products as CH_3, HCO, and CH_2CHO and their product branching ratios,[17] dominant two-body and three-body reaction pathways from these intermediates to CO and CO_2 are shown in Scheme. 1(b). Although HCHO, HCOOH, and CO molecules are detected as intermediates of final product CO_2 in this study, short lived $C_xH_yO_z$ ($x \leq 2, y \leq 3, z \leq 2$) intermediates, shown in Scheme 1, will be formed as additional intermediates in oxidation processes.

Although we detected HCOOH as an intermediate species, it was not shown in Scheme 1. Possible formation pathways of HCOOH are as follows.

$$CH_2 + O_2 \rightarrow CH_2OO \quad (19)$$
($k_{19} = 6.37 \times 10^{-11}$ cm^3 molecule^{-1} s^{-1})[17]

$$CH_3O_2 + OH \rightarrow CH_2OO + H_2O \quad (20)$$
($k_{20} = 1.65 \times 10^{-13}$ cm^3 molecule^{-1} s^{-1})[17]

$$HCO + OH \rightarrow HCOOH \quad (21)$$
($k_{21} = 9.20 \times 10^{-13}$ cm^3 molecule^{-1} s^{-1})[17]

Although OH radicals are not formed in the initial $O(^3P)/C_2H_4$ reaction (14), they will be formed during some secondary reactions and contribute to the formation of HCOOH. $O(^1D)$, OH, O_2, and O_3 are not major active species in the decomposition of C_2H_4 in the initial stage. However, they will be important oxidants for $C_xH_yO_z$ intermediates shown in Scheme 1 and reactions (20) and (21). Although 172 nm photoabsorption and photodissociation data of $C_xH_yO_z$ intermediates shown in Scheme 1 have not been known, direct VUV photodissociation processes may also take part in the photolysis processes of these intermediates.

4. Summary and Conclusion

The photolysis of ethylene by using head-on and side-on types of 172 nm Xe_2 excimer lamps was studied in N_2 or air at atmospheric pressure. We found that C_2H_4 was selectively

converted to 1-C_4H_8 in N_2, whereas C_2H_4 was oxidized to CO_2 via HCO, HCOOH, and CO in air. In the presence of O_2, $O(^3P,^1D)$ and O_3 can be active species for the removal of C_2H_4. Results showed that $O(^3P)$ is the major active species under the 172 nm photolysis of C_2H_4 and the contributions of $O(^1D)$ and O_3 are unimportant in the initial stage of the C_2H_4 decomposition. The removal rate of C_2H_4 by using the side-on lamp was 8.2 times faster than that using the head-on lamp because of larger irradiation volume in the reaction chamber. Photochemical removal of rate of C_2H_4 using the side-on lamp was 15 times faster than that of CH_4,[14] for which minor $O(^1D)$ atoms were the major active species. The present results demonstrate that mercury-free 172 nm Xe_2 excimer lamp is useful for C_2H_4 removal in air.

Acknowledgments

This work was supported by NEDO (project number NCJJ200049, 2008–2009,), and City Area Project from Fukuoka Prefecture (2009).

References

1) N. Pathak, O. J. Caleb, M. Geyer, W. B. Herppich, C. Rauh, and P. V. Mahajan, *Food Bioprocess Technol.*, 10, 982 (2017).
2) B. P. Mabusela, Z. A. Belay, B. Godongwana, N. Pathak, P. V. Mahajan, and O. J. Caleb, *Food Bioprocess Technol.*, 15, 28 (2022).
3) B. Mabusela, Z. A. Belay, B. Godongwana, N. Pathak, P. V. Mahajan, P. M. K. Mathabe, and O. J. Caleb, *S. Afr. J. Plant Soil*, 38, 347, (2021).
4) C. E. Tas, S. Hendessi, M. Baysal, S. Unal, F. C. Cebeci, Y. Z. Menceloglu, and H. Unal, *Food Bioproc. Tech.*, 10, 789 (2017).
5) E. Feliziania, G. Romanazzia, and J. L. Smilanick, *Postharvest Biol. Technol.*, 93, 38 (2014).
6) F. Aprilliani, E. Warsiki, and A. Iskandar, In: *IOP Conference Series: Earth Environmental Science*, p. 012003 (2018).
7) N. Pathak, O. J. Caleb, C. Rauh, and P. V. Mahajan, *Biosyst. Eng.*, 159, 33 (2017).
8) B. P. Mabusela, Z. A. Belay, B. Godongwana, O. J. Caleb. *J. Food Sci. Technol.*, 60, 2557 (2023).
9) M. Tsuji, T. Kawahara, N. Kamo, and M. Miyano, *Bull. Chem. Soc. Jpn.*, 83, 582 (2010).
10) M. Tsuji, T. Kawahara, K. Uto, N. Kamo, M. Miyano, J. Hayashi, and T. Tsuji, *Environ. Sci. Pollut. Res.*, 25, 18980 (2018).
11) M. Tsuji, M. Miyano, N. Kamo, T. Kawahara, K. Uto, J. Hayashi, and T. Tsuji, *Environ. Sci. Pollut. Res.*, 26, 11314 (2019).
12) M. Tsuji, T. Kawahara, K. Uto, J. Hayashi, and T. Tsuji, *Engineering Sciences Reports, Kyushu University*, 41, 1 (2019).
13) M. Tsuji, M. Miyano, N. Kamo, T. Kawahara, K. Uto, J. Hayashi, and T. Tsuji, *Int. J. Environ. Sci. Technol.*, 16, 7229 (2019).
14) M. Tsuji, N. Kamo, M. Miyano, and M. Kawahara, *Engineering Sciences Reports, Kyushu University*, 46, 19 (2024).
15) H. Okabe, "*Photochemisty of Small Molecules*", John Wiley & Sons, New York (1978).
16) J. B. Nee and P. C. Lee, *J. Phys. Chem. A*, 101, 6653 (1997).
17) *NIST Chemical Kinetics Database on the Web, Standard Reference Database 17, Version 7.1 (Web Version)*, Release 1.6.8, Data Version 2024. http://kinetics.nist.gov/kinetics/index.jsp.
18) D. M. P. Holland, D. A. Shaw, M. A. Hayes, L. G. Shpinkova, E. E. Rennie, L. Karlsson, P. Baltzer, and B. Wannberg, *Chem. Phys.*, 219, 91 (1997).
19) *NIST Chemistry WebBook, NIST Standard Reference Database*, Number 69, (2023) https://doi.org/10.18434/T4D303.
20) H. Hara, K. Kodama, and I. Tanaka, *Bull. Chem. Soc. Jpn.*, 48, 711 (1975).
21) B. Fu, Y.-C. Han, J. M. Bowman, F. Leonori, N. Balucani, L. Angelucci, A. Occhiogrosso, R. Petrucci, and P. Casavecchia, *J. Chem. Phys.*, 137, 22A532 (2012).
22) K. Honma, *J. Chem. Phys.* 99, 7677 (1993).
23) M. González, M. P. Puyuelo, J. Hernando, R. Martnez, R. Sayós, and P. A. Enrquez, *Chem. Phys. Lett.*, 346, 69 (2001).
24) S.-H. Lee, W.-K. Chen, and W.-J. Huang, *J. Chem. Phys.*, 130, 054301 (2009).
25) A. Miyoshi, J. Yoshida, N. Shiki, M. Koshi, and H. Matsui, *Phys. Chem. Chem. Phys.*, 11, 7318 (2009).